Beat-by-beat changes of viscoelastic and inertial properties of the pulmonary arteries

B. B. LIEBER, Z. LI, AND B. J. B. GRANT
Departments of Mechanical and Aerospace Engineering and of Medicine, State University of New York at Buffalo, Buffalo, New York 14260

Lieber, B. B., Z. Li, and B. J. B. Grant. Beat-by-beat changes of viscoelastic and inertial properties of the pulmonary arteries. *J. Appl. Physiol.* 76(6): 2348–2355, 1994.—We tested the hypothesis that pulmonary arterial input impedance varies during the ventilatory cycle due to alterations not only of the viscoelastic components of the pulmonary vasculature but also due to changes of the inertial components. A four-element lumped-parameter model was used to fit the pulmonary arterial pressure-flow recordings in the time domain in 10 anesthetized dogs. The four elements consisted of a resistor (R) that represents input resistance, a second resistor (R1) and a capacitor (C1) that represent the viscoelastic properties of the pulmonary vasculature, and an inductor (L1) that represents inertial properties of blood within the pulmonary vasculature. The parameters were evaluated at each heartbeat throughout the ventilatory cycle at three levels of positive end-expiratory pressure. All four parameters varied significantly during the ventilatory cycle. R, C1, L1, and R1 varied by up to 97, 33, 13, and 17%, respectively. Changes in parameter values were most apparent at the start of expiration when the most rapid changes of lung volume occur. This pattern of the results is consistent with the hypothesis that the time variation of pulmonary arterial impedance is due to dynamic shifts of blood volume between the extra-alveolar and alveolar arteries.

input impedance; pulmonary arterial compliance; characteristic impedance

PREVIOUSLY, WE HAVE SHOWN that pulmonary arterial compliance (Ca) was greater at the start of expiration than at the start of inspiration (5). Pulmonary arterial pressure and flow were used to calculate the pulmonary arterial input impedance. Ca was then calculated from the impedance spectrum with a lumped-parameter model. Only two instances during the ventilatory cycle were studied because of limitations imposed by the method of calculating the parameters with the frequency domain approach. Fourier analysis requires pressure (and flow) to be equal at the beginning and end of each cardiac cycle during the ventilatory cycle. In this report, we hypothesize that all components of the input impedance may be varying during the ventilatory cycle but they may not have been identified previously because we were limited to two specific phases of the ventilatory cycle. This matter is of importance because time variation of input impedance would impose severe restrictions on the conditions under which it is measured.

To test this hypothesis, we developed a new method for estimating the parameters of the lumped model at every heartbeat throughout the ventilatory cycle. We calculated the parameter values of the same four-element lumped-parameter model directly from the pressure and flow in the time domain without the intervening step of transforming the data into the frequency domain. Previously, we postulated that the time-varying changes of Ca were due to the shifts of blood volume between the alveolar and extra-alveolar arteries (4). If this explanation is correct, we would anticipate that most of the variation of the viscoelastic and inertial components would occur during the initial expiratory phase of the ventilatory cycle when there are rapid changes of lung volume.

METHODS

Animal preparation. The experimental preparation that we used has been described in detail previously (5). Briefly, experiments were performed on 10 mongrel dogs that weighed between 17 and 21 kg. Anesthesia was induced with thiamylal (1.5 mg/kg) followed immediately by intravenous injection of 2 ml/kg body wt of a chloralose solution (6 g/dl of α-chloralose, 4.6 g/dl of sodium tetraborate, and 5 g/dl of sodium bicarbonate). Anesthesia was maintained with a continuous infusion of a 1:1.85 dilution of that solution at a rate of 1.32 $ml \cdot kg^{-1} \cdot h^{-1}$. The dogs were intubated and ventilated with a volume-cycled pump (model 681, Harvard Apparatus, Natick, MA). Intravenous pancuronium bromide (0.1 mg/kg) was used for muscular paralysis. The ventilatory rate and tidal volume were constant throughout each experiment. Stroke volume of the ventilator was set at ~15 ml/kg at a rate of 12–15 min^{-1}. Inspiration was achieved by positive pressure, whereas expiration was passive. The duration times of inspiration and expiration were fixed and equal. Airway gas fractions were monitored with a Perkin-Elmer mass spectrometer. Airway pressure was monitored with a Validyne differential pressure transducer. A catheter was placed in the right femoral artery to monitor systemic arterial pressure with a Statham P23 ID pressure transducer.

The chest was open through a left thoracotomy in the fifth intercostal space, and 5 cmH_2O of positive end-expiratory pressure (PEEP) were applied to prevent atelectasis. The pericardium was then transected vertically, and the pulmonary artery was isolated by blunt dissection. A Statham electromagnetic flow probe (between 16 and 18 mm ID) was placed around the main pulmonary artery. Two 3F micromanometer-tipped catheters (Millar, Houston, TX) were placed, through purse-string sutures, into the right ventricular outflow tract and into the pulmonary artery for simultaneous pressure measurements. All pressure calibrations were performed relative to atmospheric pressure. After the animals were instrumented, data collection was started when the preparation was judged to be stable as manifested by constant mean systemic pressure, pulmonary arterial pressure, and flow. In all dogs, measurements were collected over a period of 10 breaths at 5, 10, and 15 cmH_2O of PEEP.

Data collection and analysis. All the collected analog signals were displayed on an eight-channel Gould 2800S strip chart recorder. All the analog signals were digitized (Data Translation DT2801A) and stored on a computer (Wells-American A Star, Columbia, SC) for off-line analysis. Data available from 7 of the 10 dogs have been published previously but only from selected points of the ventilatory cycle (5). The raw data in

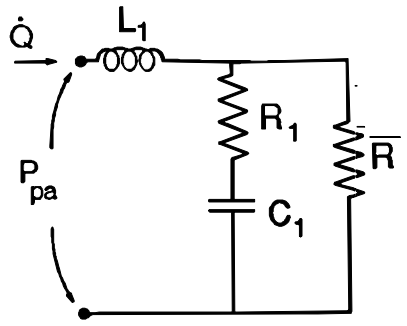

FIG. 1. Electrical analog of lumped-parameter model where capacitance represents reciprocal of elasticity, inductance represents inertia, and resistance represents mechanical viscous dissipation. R, resistor (input resistance); R1, 2nd resistor (viscoelastic property); C1, capacitor (viscoelastic property); L1, inductor (inertial property); Q̇, blood flow; Ppa, pulmonary arterial pressure.

hose experiments had been stored on magnetic tape. The data vere redigitized from the magnetic tape with an eight-channel Hewlett-Packard FM tape recorder. The sampling rate of the various pressure and flow waves was set at 500 Hz/channel. The beginning of each ventilatory cycle was recorded by using the output of a microswitch that was positioned on the ventilator and that delivered a 5-V pulse at the end of expiration. The beginning of each individual heartbeat was defined from a recorded pulse that was triggered by the QRS complex of the electrocardiogram (ECG; Biotech amplifier, Gould).

Analysis methods. A lumped-parameter model, shown in Fig. 1, was used to calculate pulmonary arterial viscoelasticity, mean pulmonary circulation resistance, and mean inertia of blood in the pulmonary circulation. The choice of this four-parameter model is discussed in detail elsewhere (7). We have changed the symbols representing the elements in the model from those that we have used previously (3–5) to reflect the entirely new analytic approach. The element R represents mean resistance, R1 and C1 represent the viscoelasticity (resistance and capacitance, respectively) of the pulmonary vasculature, and L1 represents the inertial properties of blood within the pulmonary circulation. The elements R, R1, C1, and L1 in Fig. 1 correspond to Rin, Z_c, Ca, and L described previously.

System parameters were evaluated for each cardiac cycle throughout the ventilatory cycle. New data subsets were generated from the experimental data. The ventilator and the ECG triggers were used to define the respiratory and cardiac cycles, respectively. Consecutive cardiac cycles within each ventilatory cycle were identified ($i = 1, \ldots, n$) for each ventilatory cycle ($j = 1, \ldots, 10$). For every i, cardiac cycles were collected from each of the 10 ventilatory cycles for both pulmonary arterial pressure and flow. The result was new subsets of pressure and flow data, each containing 10 cardiac cycles at particular phases of the respiratory cycle. Therefore, time variations due to ventilation in the newly constructed data sets were virtually eliminated. As a result, these sets can be considered as obtained from a system in steady-state oscillations (with no time variations) driven by a steady frequency source (Fig. 2).

The data sets were low-pass filtered using a finite impulse response frequency domain design filter with a single transition sample (11). The advantage of using this type of filter lies in the fact that it permits frequency-time domain transformations and filtering without distortion of the phase response of the filtered data. The cutoff frequency was set at a value of 10 harmonics of cardiac frequency because no important physiological signal was anticipated at frequencies higher than 10 cardiac harmonics and so it would be considered to be instrumentation noise. Furthermore, low-pass filtering eliminates the possible slight mismatch at the end of each cardiac cycle and the beginning of the next.

The system parameters were evaluated by solving the circuit equations in the time domain. The optimization of the parameters for each data set was performed using recursive quadratic programing technique. The main idea behind this type of optimization is to find the optimum solution by solving a sequence of quadratic programing subproblems that are obtained with quadratic approximations of the original problem after its Taylor series expansion. A description and the advantages of using this type of parameter optimization are described in detail else-

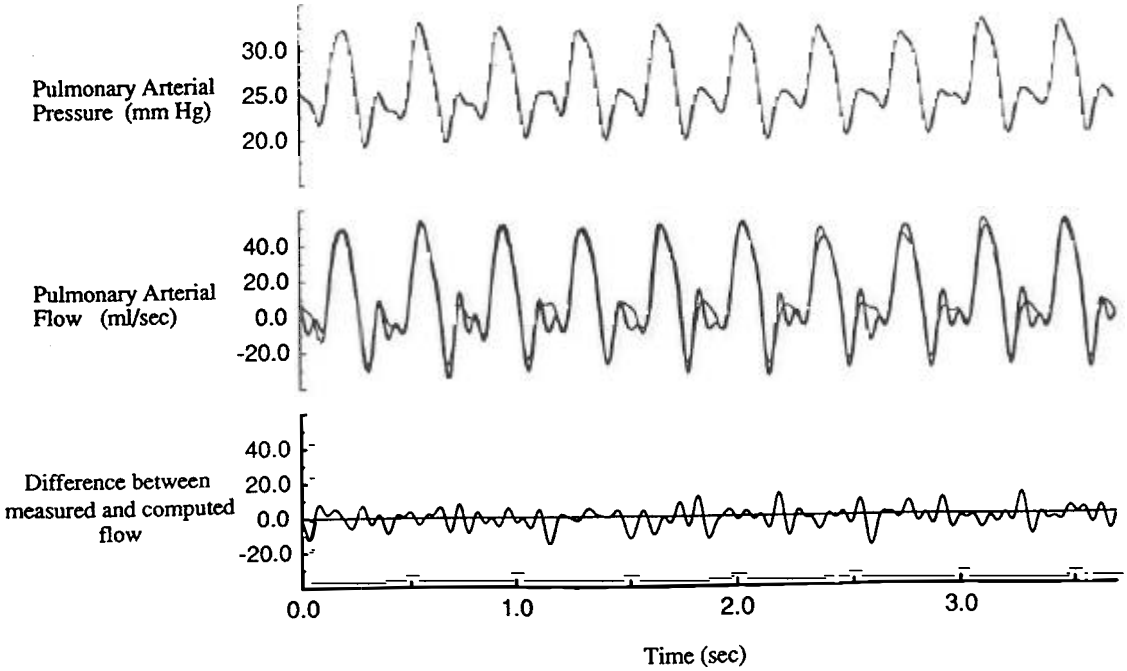

FIG. 2. Recording of quasi-stationary subset of heartbeats at beginning of expiration [positive end-expiratory pressure (PEEP) = 15 cmH_2O]. Thick line, experimental data of pressure and flow; thin line, computational fit of flow.

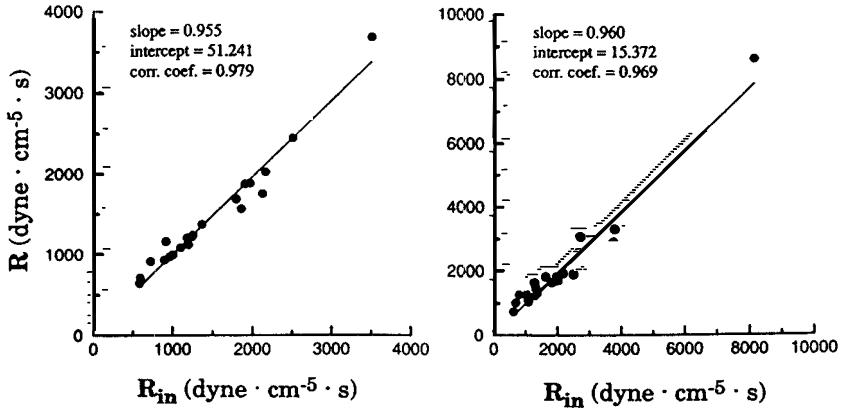

FIG. 3. Comparison of mean R derived by impedance matching (Rin from previous studies; abcissa) and time domain analysis (this study; ordinate). *Left*: start of inspiration. *Right*: start of expiration.

where (9). A typical fit generated by this procedure is shown in Fig. 2 (*middle curve*).

Statistical analysis. A detailed description of the nonparametric regression technique is provided elsewhere (8). In brief, generalized additive models were used to analyze the relationship between the parameter values during the ventilatory cycle. These models extend the more commonly used generalized linear models by replacing the linear predictors with cubic smoothing splines. These nonlinear functions are fitted to the data without presupposing any particular mathematical form. The fitting procedure is a weighted least squares approach. The weights are related to a local scoring procedure of the deviations over a limited portion of the fitted regression. Therefore, the variance around the fitted regression is not assumed to be uniform throughout the respiratory cycle. The nonlinearity in the fitted regression is dependent on the order of the model (i.e., number of degrees of freedom) allowed. The order of the model was determined by the generalized cross-validation criterion. This criterion is similar to the Akaike information criterion (8). This criterion selects the order model based on a trade-off between the least bias and minimizes the variance around the regression.

RESULTS

Seven of the 10 dogs used in this analysis were also used in our previous study (5). This enabled us to compare the direct time domain results of this study with the previous results that were obtained via the impedance spectrum. Figure 3 shows a comparison of the results for input resistance. In both cases, at the start of inspiration as well as at the start of expiration the results are in excellent agreement. The regression equations are not significantly different from the line of identity. The results for resistor R1 are depicted in Fig. 4. These results are also in good agreement at both phases of the respiratory cycle. The slopes were not significantly different from unity, and the intercepts were not significantly different from zero. Nonetheless, the results for the compliance do not compare as well. In Fig. 5, the slope of the regression line is significantly less than unity ($P < 0.001$). This result suggests that fitting the impedance spectrum in our previous study yielded considerably higher compliance values than the time domain method. Furthermore, the previous results contain high variability among dogs and among the different levels of PEEP within the same dog. The time domain results, in contrast, are more stable. For example, the three points that were off scale in Fig. 5 (*left*) are all from the same dog at three different levels of PEEP. Although the time domain results for these points are quite consistent (i.e., have similar values at all 3 levels of PEEP), the frequency domain results change >40-fold. The reason for the high variability of C1 (and the inability to evaluate the L1 in most cases) by using the impedance spectrum is due to the fact that both L1 and C1 have to be evaluated from the imaginary part of the Fourier spectrum. Within the physiological range of frequencies of the spectrum, the imaginary part is about two orders of magnitude smaller than its real counterpart, which is dominated by the input resistance. It was not possible to compare L1 with the previous study because this parameter was unobtainable in most of the cases.

The time variations in the model parameters through-

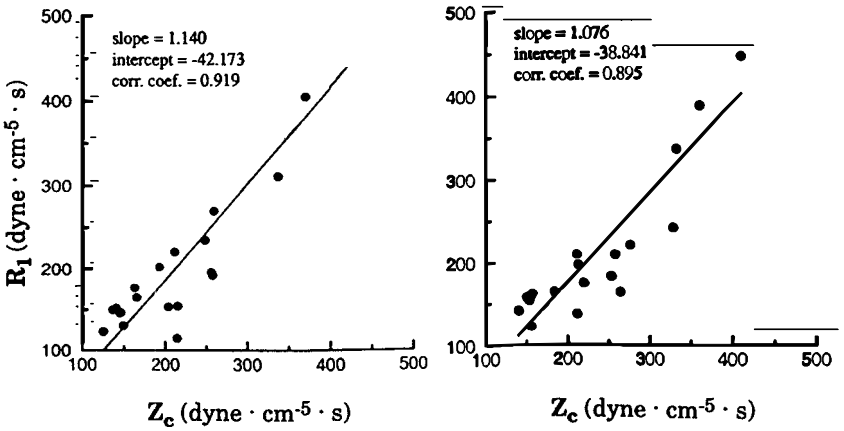

FIG. 4. Comparison of R1 derived by impedance matching (Z_c from previous studies; abscissa) and time domain analysis (this study; ordinate). *Left*: start of inspiration. *Right*: start of expiration.

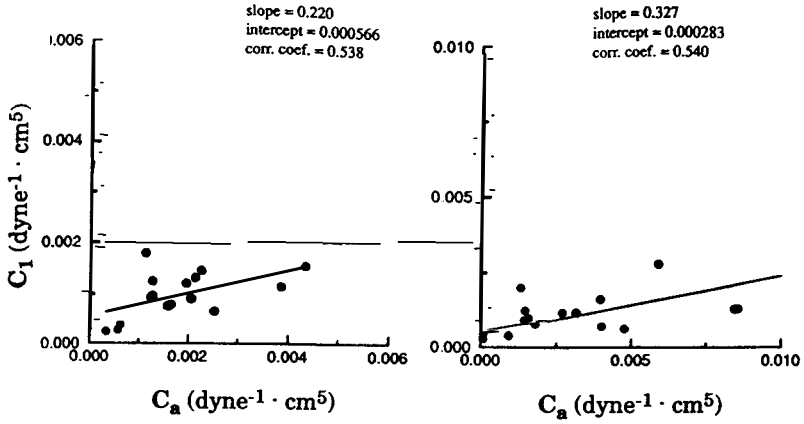

FIG. 5. Comparison of C1 derived by impedance matching (Ca from previous studies; abscissa) and time domain analysis (this study; ordinate). *Left*: start of inspiration. Three extraneous points (*x,y*) were included in analysis: (0.0048,0.011), (0.0012,0.013), and (0.045,0.013). *Right*: start of expiration. Two extraneous points were included in analysis: (0.028,0.0089) and (0.023,0.0013).

out the respiratory cycle for PEEP levels of 5, 10, and 15 cmH_2O are shown in Figs. 6, 7, and 8, respectively. The parameters, in this study, were evaluated at each heartbeat throughout the ventilatory cycle at three levels of PEEP. All four parameters varied significantly during the ventilatory cycle. R, C1, L1, and R1 varied by up to 97, 33, 13, and 17%, respectively. Changes in parameter values were most apparent at the start of expiration when the most rapid changes of lung volume occur.

Note that Figs. 6–8 show the temporal variations about the mean values except for airway pressure. Table 1 depicts the mean value of the parameters as well as the

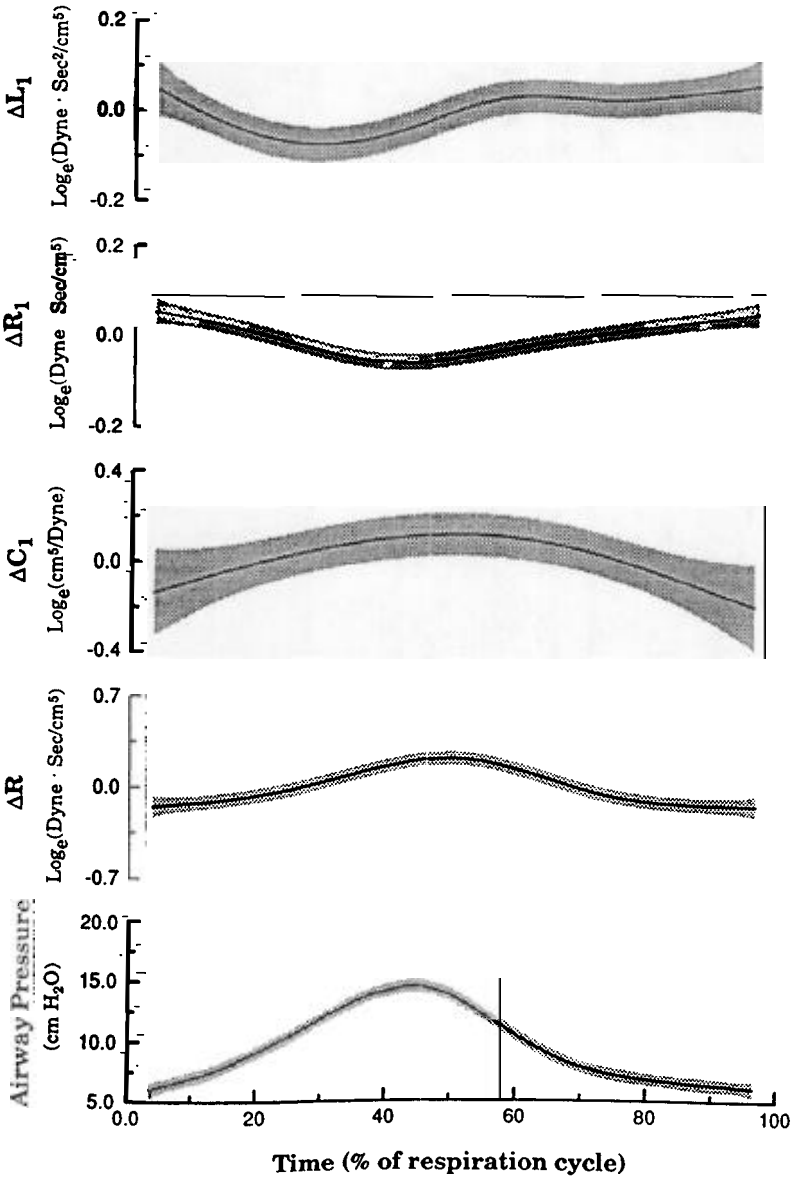

FIG. 6. Time variation of model parameters with respect to mean values during ventilatory cycle at 5 cmH_2O PEEP. Airway pressure is given in absolute values. Shaded areas, ±2SE.

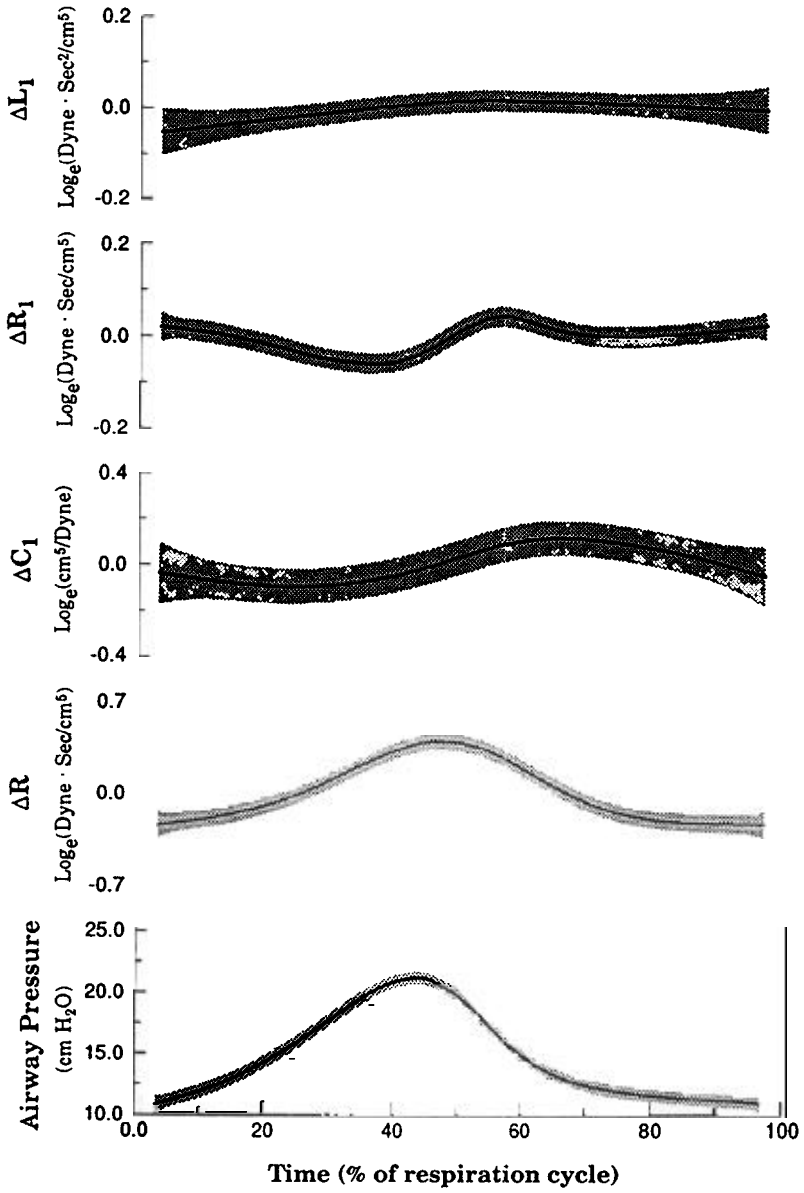

FIG. 7. Time variation of model parameters with respect to mean values during ventilatory cycle at 10 cmH_2O PEEP. Airway pressure is given in absolute values. Shaded areas, ±2SE.

number of degrees of freedom required to fit the data. The nonlinear *P* values are also given in Table 1. Only R was affected by the quasistatic changes of lung volume due to PEEP; C1, R1, and L1 were unaffected.

DISCUSSION

First, we compare the time domain approach used for parameter estimation in this study with the frequency domain approach used previously. We then discuss the implications of these new results for our hypothesis regarding the mechanism producing the time-varying hemodynamic properties of the pulmonary vasculature. Finally, we discuss the impact of our results on the concept of input impedance with regard to the pulmonary circulation.

Parameter estimation by time and frequency domain methods. Our previous approach transformed the pressure and flow data into the frequency domain (5). The lumped-parameter model is the frequency domain data with the maximum likelihood criterion (7). In the present study, the lumped-parameter model was fitted to the time domain data with the least squares criterion. What effect did these differing approaches have on the parameter values?

The mean R value and the changes between the start of inspiration and the start of expiration were similar between the present and previous approaches. This result is not surprising because R is simply mean pressure divided by mean flow; therefore no differences would be anticipated between the two approaches. Figure 3 indicates that there is close agreement: the data points are all close to the line of identity.

Figure 4 indicates that estimates of R1 are in reasonable agreement with Z_c. Previously, we found no significant changes of Z_c between the start of inspiration and the start of expiration. In the present study, R1 changes quite rapidly during this phase of respiration at 10 and 15 cmH_2O of PEEP. As a result, it is difficult to identify the precise values of R1 that occur at the start of inspiration. Therefore, we were unable to make direct comparisons.

In contrast to R and R1, there were differences be-

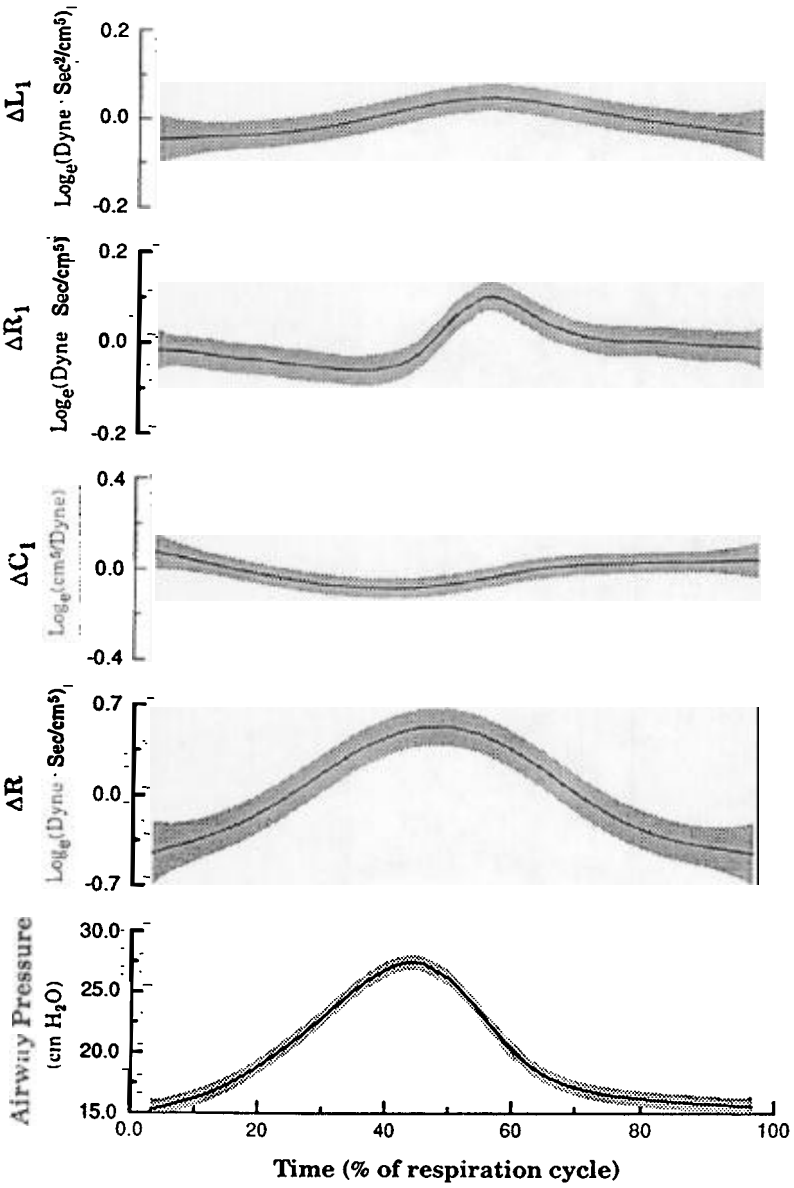

FIG. 8. Time variation of model parameters with respect to mean values during ventilatory cycle at 15 cmH_2O PEEP. Airway pressure is given in absolute values. Shaded areas, ±2SE.

tween the two methods with regard to the estimation of L1 and C1. The inertance term was defined in less than one-half of the spectra with Fourier analysis. With the time domain approach, we identified different values for L1 in 9 of the 10 dogs. In the previous study (7), the ECG signal that contaminated the flow signal, particularly during early diastole, was removed from the flow signal in the time domain and replaced by interpolation. With our present approach the ECG signal was removed from the flow signal by low-pass filtering, and in the three dogs not analyzed in the previous study, there was no contamination of the flow signal so that removal of the ECG signal was not needed. In another study, we have found that flow during early diastole has a profound effect on L1. Therefore the identification of L1 may be related to the method of eliminating the ECG contamination of the flow signal rather than the method of calculation.

Although there were no statistically significant differences between the mean C1 at the three levels of PEEP, there was a large discrepancy between the compliance term calculated by frequency (Ca) and time domain methods (C1) as indicated in Fig. 5. The estimates of the compliance term were lower and considerably less variable. In addition, the changes of C1 during the respiratory cycle were quite different from what would be anticipated from the results obtained by the frequency domain. In the frequency domain, we found that C1 was greater at the start of expiration than at the start of inspiration. The results that we obtained with the time domain study are compatible with this finding at 5 and 10 cmH_2O of PEEP, whereas the opposite result occurs at 15 cmH_2O of PEEP.

One possible explanation is that in just less than one-half of the data analyzed previously the inertance term was zero. Therefore, the lumped-parameter model became a three- rather than a four-parameter model. Because there is some interdependence between the parameter values (5), we were concerned that these differences in the parameter estimates of the compliance term may be due to differences in the number of elements used in the lumped-parameter model. However, when we eliminated the inertance term from the time domain method

TABLE 1. *Mean values of model parameters for all levels of PEEP*

	R, $dyn \cdot cm^{-5} \cdot s$	C1, $10^{-3} \cdot dyn^{-1} \cdot cm^5$	R1, $dyn \cdot cm^{-5} \cdot s$	L1, $dyn \cdot cm^{-5} \cdot s^2$
		PEEP = 5 cmH_2O		
Means	1,115 + 42 −40	1.86 + 0.21 −0.19	252.0 + 10.5 −10.2	1.82 + 0.21 −0.19
df	5	2	5	5
NLP	0.0001	0.005	0.0001	0.003
		PEEP = 10 cmH_2O		
Means	1,466 + 66 −63	1.87 + 0.21 −0.19	227.0 + 7.9 −7.7	2.05 + 0.18 −0.17
df	7	4	9	2
NLP	0.0001	0.023	0.0001	0.085
		PEEP = 15 cmH_2O		
Means	2,738 + 238 −219	1.89 + 0.22 −0.19	229.0 + 7.1 −6.9	2.22 + 0.20 −0.18
df	5	4	10	4
NLP	0.0001	0.002	0.0001	0.002

Values are means +SE or −SE. R, mean resistance; R1 and C1, resistance and capacitance of pulmonary vasculature, respectively; L1, inertial properties of blood; PEEP, positive end-expiratory pressure; df, degrees of freedom needed for the fit; NLP, *P* value for nonlinear component of fit.

and recalculated C1, the mean levels of C1 and the variation of C1 were similar to the four-element model. Therefore, we believe that the differences between the frequency and time domain methods of parameter estimation are related to the different methods of calculation rather than differences in the effective number of parameters in the model. The smaller variability of the compliance estimates with the time domain approach suggests that the variation of the compliance term during the respiratory cycle is likely due to the instability of the compliance estimates with the frequency domain approach.

The success of the time domain approach over the frequency domain approach is that lumped-parameter estimates can be obtained throughout the respiratory cycle and that the parameter estimates are more stable than with the frequency domain approach. The disadvantage of the time domain approach is that it only provides a lumped-parameter estimate of the impedance spectrum and not the impedance spectrum itself.

Implications for the measurement of pulmonary input impedance. The fact that the lumped parameters are time varying indicates that pulmonary input impedance is also time varying. One approach is to confine estimation of impedance during spontaneous breathing as we have done previously. This approach provides a first approximation of the impedance spectrum but by definition it is limited to a specific phase of respiration. Another approach is to suspend ventilation as a specific phase of the ventilatory cycle. This approach has the same limitations, but in addition arterial blood gas composition is varying continuously even during breath holding (1). These small variations of arterial blood gas composition could provoke responses directly through the bronchial circulation (10) or reflexly through the carotid body (2). Furthermore, there is no specific phase of the respiratory cycle that consistently represents the mean values of the parameters, although the start of inspiration is a reasonable estimate.

Previously we suggested a time-varying compliant element to circumvent this problem. The results of the present study indicate that this approach would be insufficient because all the elements of the lumped-parameter model are time varying. Another approach would be to introduce the respiratory pressure changes as an input to the systems and determine whether the parameter values then become time invariant. Pilot studies indicate that this approach is feasible (6).

Cause of time-varying pulmonary hemodynamics. Previously, we hypothesized that the cause of the time-varying changes of pulmonary arterial input impedance is due to shifts of blood volume between the alveolar and extra-alveolar arteries during the respiratory cycle. The caliber of the alveolar vessels is related inversely to alveolar pressure. In contrast, the caliber of the extra-alveolar vessels is related directly to transpulmonary pressure. Therefore during inspiration, as lung volume increases, the alveolar vessels decrease in volume as they are compressed by the increasing alveolar pressure and stretched by increasing lung volume. In contrast, the extra-alveolar vessels increase in volume as lung volume and transpulmonary pressure increase. Thus, there must be a dynamic shift of blood volume from the extra-alveolar to the alveolar arteries during expiration. The fact that there were no changes in the mean levels of R1, C1, and L1 with steady-state changes of airway pressures due to PEEP supports the theory that the time-varying changes during the respiratory cycle are related to dynamic rather than static shifts of blood volume.

Three elements of the lumped-parameter model modulate the pulsatile components of flow: R1, C1, and L1. R1 showed the greatest changes with respiration. Most of the changes in R1 occurred close to the start of expiration. This pattern was be seen at 15 cmH_2O PEEP, to a lesser extent at 10 cmH_2O PEEP, and was absent at 5 cmH_2O PEEP. The fact that most of these changes occurred close to the start of expiration is in accord with our hypothesis. Although both L1 and C1 varied with the respiratory cycle, this pattern of change was not observed. Because of these differences between parameter estimates and between the previous and the present method of calculation, the precise physiological representation of these parameters cannot be assumed from our previous work (7).

The measured changes in R1 might be expected to be the net result of these two competing effects. On the one hand, our hypothesis predicts a shift in blood volume from the alveolar to the extra-alveolar arteries against the direction of flow. Therefore, this shift would increase the opposition to pulsatile flow and therefore increase characteristic impedance to the extent that R1 represent characteristic impedance. On the other hand, characteristic impedance would be expected to decrease because of the increasing pulmonary arterial pressure distending the pulmonary arteries during inspiration. Therefore the changes in R1 do conform to our prediction. However, the precise physiological representation of these parameters cannot be assumed from our previous work (7) because the present method of parameter estimation differs radically from our previous method. The respiratory variations of L1 and C1 with increasing levels of

PEEP are less consistent than the changes of R1. Therefore, it is difficult to determine the physiological interpretation of these changes.

Nevertheless, the general pattern of parameter changes varied as we had anticipated from our hypothesis. First, there were no significant changes of the elements (R1, C1, and L1) with increasing levels of PEEP. Second, the components that control the pulsatile components of flow varied during the respiratory cycle. Third, most of the respiratory variation of R1 occurred close to the start of expiration, although this pattern was not apparent for C1 or L1. These results support the hypothesis that time variation of impedance is related to shifts in blood volume between the extra-alveolar and alveolar arteries.

This work was supported in part by the National Heart, Lung, and Blood Institute Grant RO1-HL-41011.

Address for reprint requests: B. Lieber, Dept. of Mechanical and Aerospace Engineering, State Univ. of New York at Buffalo, Buffalo, NY 14260.

Received 3 May 1993; accepted in final form 18 January 1994.

REFERENCES

1. **Cross, B. A., B. J. B. Grant, A. Guz, P. W. Jones, S. J. G. Semple, and R. P. Stidwell.** Dependence of phrenic motoneurone output on its relationship to the respiratory oscillations of arterial blood gas composition. *J. Physiol. Lond.* 290: 163–184, 1979.
2. **Downing, S. E., and J. C. Lee.** Nervous control of the pulmonary circulation. *Annu. Rev. Physiol.* 42: 199–210, 1980.
3. **Fitzpatrick, J. M., and B. J. B. Grant.** Effects of pulmonary vascular obstruction on right ventricular afterload. *Am. Rev. Respir. Dis.* 141: 944–952, 1990.
4. **Grant, B. J. B., and J. M. Canty, Jr.** Effect of cardiac output on pulmonary hemodynamics. *Respir. Physiol.* 76: 303–318, 1989.
5. **Grant, B. J. B., J. M. Fitzpatrick, and B. B. Lieber.** Time-varying pulmonary arterial compliance. *J. Appl. Physiol.* 70: 575–583, 1991.
6. **Grant, B. J. B., Z. Li, and B. B. Lieber.** Modeling of pulmonary hemodynamics. In: *1992 Advances in Bioengineering*, edited by M. W. Bidez. New York: ASME, 1992, vol. 22, p. 207–210.
7. **Grant, B. J. B., and L. J. Paradowski.** Characterization of pulmonary arterial input impedance with lumped parameter models. *Am. J. Physiol.* 252 (*Heart Circ. Physiol.* 21): H585–H593, 1987.
8. **Hastie, T. J., and R. J. Tibshirani.** *Generalized Additive Models.* New York: Chapman & Hill, 1990, p. 136–173.
9. **Li, Z., and B. B. Lieber.** Estimation of organ transport function: model-free deconvolution by recursive quadratic programing optimization. *J. Biomech. Eng.* 114: 482–489, 1992.
10. **Marshall, B. E., C. Marshall, M. Magno, P. Lilagan, and G. G. Pietra.** Influence of bronchial arterial Po_2 on pulmonary vascular resistance. *J. Appl. Physiol.* 70: 405–415, 1991.
11. **Oppenheim, A. V., and R. W. Schafer.** *Digital Signal Processing.* Englewood Cliffs, NJ: Prentice-Hall, 1975, p. 252.